IJTBI
International Journal of Technovation and Business Insights
Volume 02, Issue 01, January-March 2026
ISSN: 3107-7900, P.CODE: 26/2-1/25
DOI: https://doi.org/10.5281/zenodo.19143413

WAVELENGTH-SELECTIVE OPTICAL EDGE FILTER DESIGN FOR THREE-RAYLEIGH-LINE DETECTION SYSTEMS

[#1]**BANDI ANUSHA,** ***Research Scholar,***
[#2]**Dr. HITESH KUMAR,** ***Research Supervisor,***
Department of Physics,
NIILM University, Kaithal, Haryana, India.

ABSTRACT: This research builds and simulates a wavelength-selective optical edge filter for three Rayleigh-line detection systems employing 405 nm, 532 nm, and 633 nm excitation wavelengths. A multilayer thin-film filter was built using QWS and optical matrix techniques in Octave software, using low and high refractive index materials (Si and MoS_2). The best wavelength transmission and separation was with a 24-layer 12HL glass frame. Simulations show cut-on wavelengths of 408.11, 536, and 640.25 nm, with variations of 0.2, 1.7, and 1.15 nm. These are close the Rayleigh wavelengths needed. Modulation transfer efficiency (MET) ratings of 32.3%, 31.3%, and 32% suggest the filters can send signals and separate wavelengths. They observed that Raman spectroscopy and optical Rayleigh line detectors benefit from multilayer edge filters. Selects wavelengths precisely and transmits effectively.

Keywords*: Optical filter; cut-onwavelength; minimum effective transmission.*

1. INTRODUCTION

The rapid expansion of analytical equipment, clinical chemistry, fluorescence operations, microscopes, Raman spectrometers, and machine vision inspections has led to the development of advanced optical filters. Band pass, low pass, high pass, and band stop filters are currently available on the market.

Optical displays are manufactured using two primary procedures. The initial approach capitalizes on the inherent capacity of materials to absorb light in order to absorb a spectrum. An absorption screen that is susceptible to heat undergoes immediate degradation. Other adverse consequences are precipitated by light pollution. The creative license of filter design is advantageous to thin film filters. Materials with varying refractive indices are employed in multi-layer interference filters. The wavelength squared is directly proportional to the thickness of any material. The efficacy of these optical screens is contingent upon the refractive index, thickness, and number of layers.

A diverse array of materials can be demonstrated to be superior on MTF displays. Performance necessitates the use of MTF filters. They promote wavefront flow, reduce attenuation, reflect, and flatten. Thin films possess multiple facets as a result of material pressure. MTF is present in anti-reflective coatings, optical files, solar cells, optical filters, and telecommunications components.

International Journal of Technovation and Business Insights
Volume 02, Issue 01, January-March 2026
ISSN: 3107-7900, P.CODE: 26/2-1/25
DOI: https://doi.org/10.5281/zenodo.19143413

The MTF filter is constructed using the quarter-wave stack (QWS) method. It is indispensable in the context of optical displays. The filter is composed of numerous layers of insulators with varying electrical conductivities. Models of quantum well states are necessary for thin-film displays that are composed of varying refractive indices. One optical wavelength can be reflected by a quarter of an optical wavelength. Despite its simplicity, the quarter wave stack is user-friendly and adaptable.

Sol-gel techniques, heat evaporation, spray pyrolysis, and RF magnetron sputtering have all been employed to develop QWS models with MTF filtering. Optical filters can be customized in terms of thickness, number of layers, transmission precision, and cut-on/cut-off range by modifying the model. Octave is employed to generate an MTF filter in this investigation. The application is equipped with a user-friendly interface, robust support for complex numbers, and straightforward code integration.

QUARTER-WAVESTACK

The utilization of quarter-waves is essential for the production of narrow film screens. The structure is composed of layers with varying lengths and refractive indices, H and L, as per M.A. Butt et al. (2017). High-pass, band-stop, and low-pass filters are all well-known to the general public.Furthermore, it is employed on laser mirror surfaces that are exceedingly lustrous.

2. EDGE FILTERS

In an edge filter, it is easy to distinguish between a rejection zone and a transmission area. The two main types of edge filters that are utilized are short wave pass (SWP) and long wave pass (LWP). The way the structure functions could depend on a number of different approaches and could seem different. The edge filters clearly delineate the transmission and reflection domains. The filters are basically a modified quarter wave stack, and their spectral areas are defined by interference instead of absorption. Because edge filters efficiently shift to shorter wavelengths as the angle of incidence increases, they are a superb technique for accurately altering the cut-on/cut-off wavelength. Unlike color glass filters, they can alter the path of a certain wavelength band, function in the 400–1000 nm range, and intensify the alteration. Transmission above a specific wavelength is enhanced by the long-pass (LP) filter, whereas transmission below that wavelength is decreased (Fig. 1).

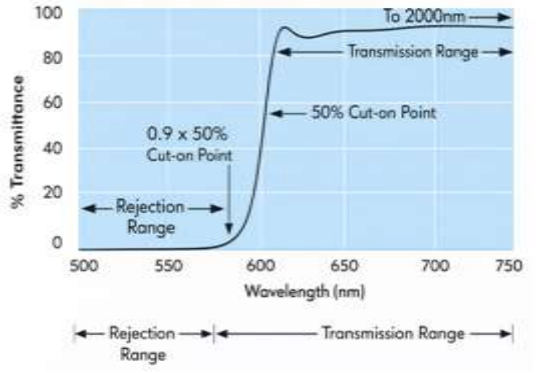

Fig. 1 Long wave pass Edge filter

Usually, a quarter-wave stack that alternates between transmission and reflection serves as the foundation for these designs. Light-absorbing materials are sometimes used to raise the optical density of the non-reflective (rejection) band of the filter. Wavelengths are reduced to about 1.3 wavelengths using short-pass edge filters. These filters are used to purify

International Journal of Technovation and Business Insights
Volume 02, Issue 01, January-March 2026
ISSN: 3107-7900, P.CODE: 26/2-1/25
DOI: https://doi.org/10.5281/zenodo.19143413

the system's laser source side. In the absence of laser lines or plasma with wavelengths shorter than the major line used, they work well as clean-up screens. They improve transmission by removing the laser "tail" on the long wavelength side of the laser line, as opposed to laser line filters. As shown in Figure 2, the short-pass (SP) filter is intended to increase transmission below a particular wavelength and decrease transmission above that threshold.

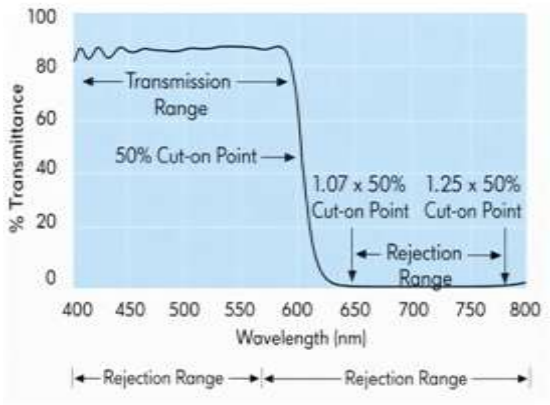

Fig. 2 Short wave pass Edge filter

Wavelengths longer than the filter's cut-off wavelength can be transmitted through long-pass filters. Long-pass edge filters are used in many industrial and biological science applications, including microscopy and fluorescence devices, to separate certain light wavelengths. Long-pass and short-pass edge filters can be used to produce custom band-pass filters. Some long-pass edge filters can act as cold mirrors to avoid overheating when exposed to infrared light.

3.EFFECT OF NUMBER OF LAYERS IN DESIGN OPTICAL FILTER

Materials with varying refractive indices are employed in multi-layered optical thin-film devices. Any layer hierarchy must have both lower (L) and higher (H) values in order to function properly. The units of micrometers (μm) and nanometers (nm) are alternated to distinguish between the various layer diameters. Vaida, Birdeanu, and Birdeanu demonstrate the feasibility of layered filters in their 2019 study.

The concept: The extreme fragility of glass results in its disintegration into a multitude of small fragments upon impact or cracking.

The number of layers in multilayer optical filters enables them to differentiate between transmission and reflection. The transmittance or reflectance is more easily altered as the number of layers increases.

EQUATIONS FOR MULTILAYER THIN FILM (MTF) ASSEMBLY OPTICAL FILTER DESIGN

The optical characteristics of the strata below are detailed in this matrix. The properties of the electric and magnetic fields are altered by the mathematical matrices that are generated by each stratum. The transmittance or reflectance coefficient can be determined by quantifying the quantity of light that penetrated the base and impact medium and reached the thin-film surface.

$$\begin{bmatrix} E \\ H \end{bmatrix} = M \begin{bmatrix} 1 \\ \eta_s \end{bmatrix} \qquad (1)$$

Vectors E and H, matrix M, and electric and magnetic fields were selected.

International Journal of Technovation and Business Insights
Volume 02, Issue 01, January-March 2026
ISSN: 3107-7900, P.CODE: 26/2-1/25
DOI: https://doi.org/10.5281/zenodo.19143413

$$\begin{bmatrix} E_a \\ H_a \end{bmatrix} = \begin{bmatrix} \cos\delta & i\sin\delta/\eta_1 \\ i\eta_1\sin\delta & \cos\delta \end{bmatrix} \begin{bmatrix} \cos\delta_2 & i\sin\delta_2/\eta_2\cos\delta_2 \\ i\eta_2\sin\delta_2 & \cos\delta_2 \end{bmatrix} \begin{bmatrix} 1 \\ \eta_3 \end{bmatrix} \quad (2)$$

$$M_r = \begin{bmatrix} 1 \\ \eta_s \end{bmatrix} \begin{bmatrix} \cos\delta r & \frac{i}{\eta}\sin\delta r \\ i\eta_s\sin\delta r & \cos\delta r \end{bmatrix} \quad (3)$$

$$M = M_L M_{L-1} \dots . Mr . M_2 M_1 r \dots M\_2M\_1 \quad (4)$$

The 2x2 grid M displays the r[th] thin film of the system. Since its inception, the strategy has remained unchanged.

$$\begin{bmatrix} B \\ C \end{bmatrix}$$

In actuality, the term "standard matrix assembly" refers to a predetermined sequence of procedures that must be executed precisely as specified. The standardized electric field of the front contact can be determined using the B(E) method. The symbol C(H) represents the standard magnetic field of the front contact. Most importantly,

$$(\delta i)\text{i})\text{f}$$

A number of layers are generated by

$$\delta r = \frac{2\pi}{\lambda} nidicos\phi r = 2\pi/\lambda nidicos\phi$$

$$\delta_r = \left(\frac{2\pi}{\lambda}\right) d_r (n_r^2 - k_r^2 - n_o^2 \cos^2 v_o - 2in_r k_r)^{1/2} \quad (5)$$

$$\eta_p = \frac{n}{cos\phi} \text{ for P- polarization} \quad (6)$$

$$\eta_S = ncos\phi \text{ for S- polarization} \quad (7)$$

And also

$$\rho = \left[\frac{\eta_o - Y}{\eta_o + Y}\right] = \eta_o - Y/\eta_o + Y \text{ but } Y \text{ is admittance of multilayer thin film}$$

$$\Gamma = \frac{B}{C} = \frac{\eta_o \cos\delta + \eta_1 \sin\delta}{\cos\delta + ((\eta_s/\eta_1)\sin\delta} \quad (8)$$

$$R = \rho\rho^* = \rho\rho r \rho^{\wedge *} \rho\rho^{\wedge *} = \left[\frac{\eta_o - Y}{\eta_o + Y}\right] \left[\left[\frac{\eta_o - Y}{\eta_o + Y}\right]\right]^* \quad (9)$$

the amplitude of the reflectance coefficient is reprenting by ρ

(9)

$$T = \frac{4\eta_o Re(\Gamma)}{(\eta_o + Y)(\eta_o + Y) + Y)} \quad (10)$$

$$(cm^{-1}) = \frac{10^7}{\lambda ex(nm)} - \frac{10^7}{\lambda(nm)} \quad 10^7/\lambda ex(nm) - \quad (11)$$

4. RESULTS AND DISCUSSION

The software is capable of operating within a wavelength range of 300 to 1000 nm and includes three distinct edge filters. The wavelengths of 405 nm, 532 nm, and 633 nm are the most prominent, and they are arranged in that order. Cases I, II, and III now represent the three distinct situations. The total number of levels remains unaffected by the plotting of wavelength versus transmission and reflectance. All of Raman's concepts

Case I: Edge Filter of Rayleigh Wavelength (λ_{ex})405 nm

Table 2 illustrates the anticipated thickness of the Si and MoS2 layers, as well as the recommended composition of the glass basal layer. The image illustrates the transmittance and reflectance curves.

Table 1. Target Value of, λ_{cut-on} and $\lambda_{cut-off}$ correspond to different λ_{ex} for simulation

S/N	λ_{ex} (nm)	Target λ_{cut-on} (nm) corresponds to 200 cm^{-1} Raman shifts.	Target $\lambda_{cut-off}$ (nm) corresponds to 4000 cm^{-1} Raman shifts
1	405	408.31	483.29
2	532	537.70	675.81
3	633	641.10	847.67

International Journal of Technovation and Business Insights
Volume 02, Issue 01, January-March 2026
ISSN: 3107-7900, P.CODE: 26/2-1/25
DOI: https://doi.org/10.5281/zenodo.19143413

Table 2. Calculated thickness of individual layer of MoS_2 and Si for filter correspond to λ_{ex} = 405 nm

Number of layers	Materials	Thickness (nm)
Air		
24	Si	32.64
23	MoS_2	21.54
2	Si	32.64
1	MoS_2	21.54
Substrate		

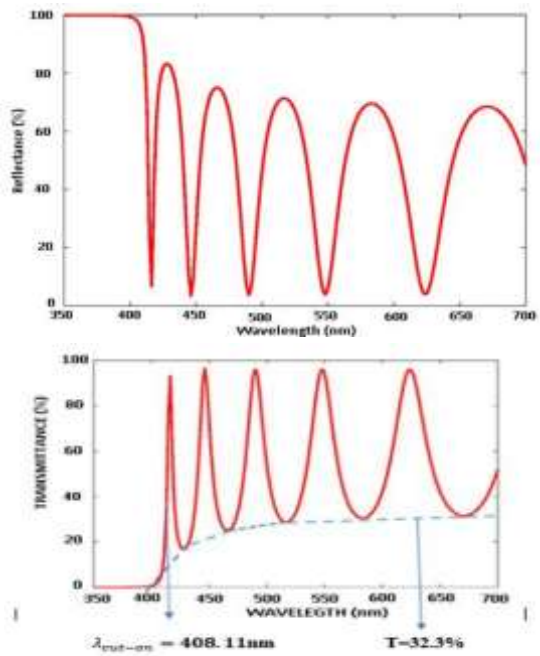

Fig. 1. Reflectance and transmittance against λλfor λ_{ex} = 405 nm

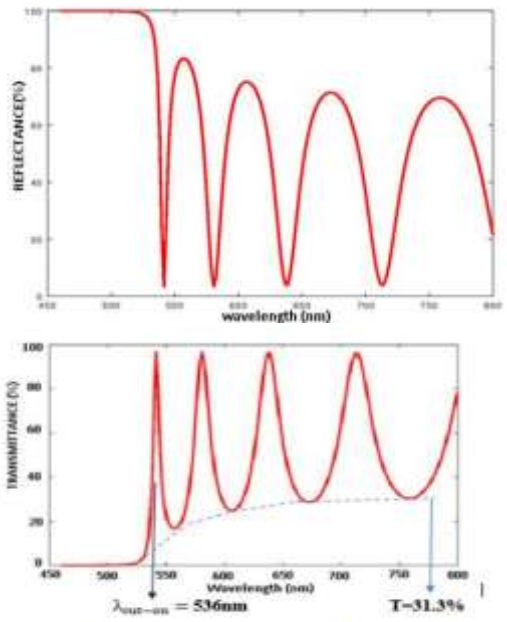

Fig. 2. Reflection and transmittance against λ for λ_{ex} = 532 nm

The MTF edge filter effectively employs it. The right-hand reflection is captivating, despite its severe distortion.

$$\lambda_{cut-on} \text{ and } \lambda_{cut-off}$$

700 nm and 408.11 nm are two potential wavelengths for measurement. The results indicate that the filter's mean efficiency of transfer (MET) is 33%.

Case II: Edge Filter of Rayleigh Wavelength of 532nm

Table 3 illustrates the thickness of each layer in the glass-based method. The correlation between reflectance and transmittance is illustrated in Figure 2. an effect that separates the various components of an image.

$$\lambda_{ex} = 532 \text{ nm},$$

$$\lambda_{cut-on} = 536 \text{ nm and } \lambda_{cut-off} = 800 \text{ nm}.$$

It successfully completed the mean efficiency test (MET) with a score of 31.3%.

Case III: Edge Filter of Rayleigh Wavelength of 633 nm

Table 4 displays the thickness of each layer using the same materials and number of layers as previously. The final product is the edge filter depicted in Figure 3.

$$\lambda_{ex} = 633 \text{ nm with } \lambda_{cut-on}$$

$$\lambda_{cut-off}$$

It was detectable within the precise range of 640.25 to 1000 nm. The MET for this filter is 32%.

Table 3. Calculated thickness of individual layer of MoS_2 and Si for filter correspond to λ_{ex} = 532 nm

Number of layers	Materials	Thickness (nm)
Air		
24	Si	36.93
23	MoS_2	27.34
2	Si	36.93
1	MoS_2	27.34
Substrate		

International Journal of Technovation and Business Insights
Volume 02, Issue 01, January-March 2026
ISSN: 3107-7900, P.CODE: 26/2-1/25
DOI: https://doi.org/10.5281/zenodo.19143413

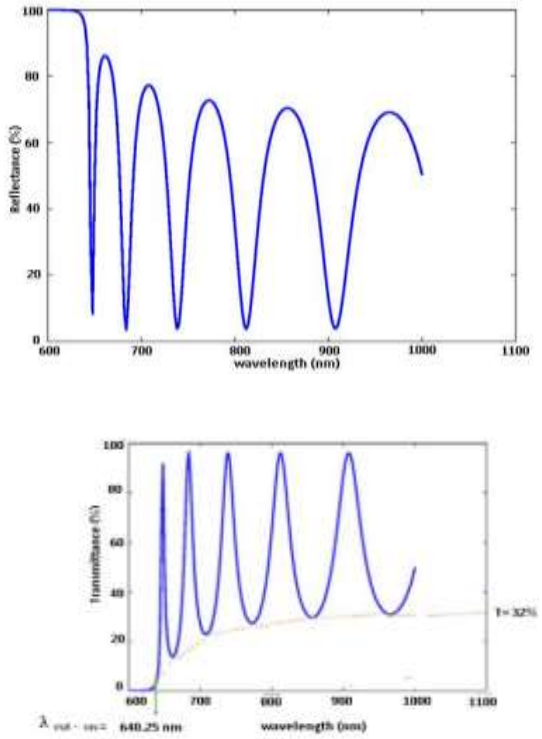

Fig. 3. Reflection and transmittance against λ for $\lambda_{ex} = 633$ nm

Table 4. Show layer thickness of 633 nm edge filter

Number of layers	Materials	Thickness (nm)
Air		
24	Si	49.61
23	MoS_2	34.50
2	Si	49.61
1	MoS_2	34.50
Substrate		

Table 5. Show λ_{cut-on} and $\lambda_{cut-off}$ edge filter λ_{ex} 405 nm, 532 nm and 633 nm

S/N	λ_{ex} (nm)	λ_{cut-on} (nm)	$\lambda_{cut-off}$ (nm)
1	405	408.11	700.00
2	532	540.00	800.00
3	633	640.25	1000.00

Each of the three edge displays serves a unique purpose.

λ_{cut-on} and $\lambda_{cut-off}$

Each individual possesses unique personality traits. The data in Table 5 was extracted using three distinct filters.

5. CONCLUSION

To construct and model wavelength-selective optical edge filters, this investigation implemented optical matrix techniques and Octave's Quarter-Wave Stack (QWS). The molybdenum disulfide (MoS_2) and silicon (Si) multilayer thin-film structure effectively captured the 405 nm, 532 nm, and 633 nm Rayleigh bands. The filter design's exceptional accuracy and reliability were demonstrated by the virtually nonexistent simulated cut-on wavelength errors of approximately 0.2 nm, 1.7 nm, and 1.15 nm. Additionally, the efficient wavelength transmission and discrimination were demonstrated by modulation transfer efficiency (MET) values ranging from 31% to 32%. The results indicate that the proposed multilayer edge filter design offers optimal optical performance, wavelength selectivity, and reliable transmission qualities. The novel optical edge filters are extremely advantageous for optical sensing systems such as Raman spectroscopy that require precise Rayleigh-line filtering and improved spectrum performance.

REFERENCES

1. Butt MA, Fomchenkov SA, Ullah A, HabibM, Ali RZ, Butt A, "Modelling of multilayerdielectric filters based on TiO 2 / SiO 2 andTiO 2 / MiF 2 for fluorescence microscopyimagingM.A.Buttetal."Comput.Opt.2016;40(5):3–7.
2. ElyutinVV, ButtMA,Khonina SN. "Coldmirror based on High-Low-High refractiveindexdielectricmaterials,"in

International Journal of Technovation and Business Insights
Volume 02, Issue 01, January-March 2026
ISSN: 3107-7900, P.CODE: 26/2-1/25
DOI: https://doi.org/10.5281/zenodo.19143413

3ndinternationalconference'.InformationTechnology and Nanotechnology. 2017;1:5–9.

3. Piegari A, Flory F, Optical thin films andcoatings:Frommaterialstoapplications.Unitedkingdom: Elsevier;2013.
4. Ng RC, Garcia JC, Greer JR,FountaineKT,"Polarization-independent,narrow-band,near-irspectralfiltersviaguidedmoderesonancesinultrathina-sianopillararrays".ACSPhotonics;2019.
5. NazarA,AliAH,JasemNA,"Newconstructionstacksfor optimizationdesignsofedgefilternewconstructionstacksforoptimizationdesignsofedgefilter."2016;8(3).